DOI: 10.1002/((please add manuscript number))
Article type: Communication

Polymer-Stabilized Micro-Pixelated Liquid Crystals with Tunable Optical Properties Fabricated by Double Templating

Yuji Sasaki, Motoshi Ueda, Khoa V. Le, Reo Amano, Shin Sakane, Shuji Fujii, Fumito Araoka, and Hiroshi Orihara*

Dr. Y. Sasaki, M. Ueda, R. Amano, S. Sakane, Dr. S. Fujii, Prof. H. Orihara
Division of Applied Physics, Faculty of Engineering, Hokkaido University
North 13 West 8, Kita-ku, Sapporo, Hokkaido 060-8628, Japan
E-mail: yuji.sasaki@eng.hokudai.ac.jp
Dr. K. V. Le, Dr. F. Araoka
RIKEN Center for Emergent Matter Science
2-1 Hirosawa, Wako, Saitama 351-0198, Japan
Dr. K. V. Le
Department of Chemistry
Faculty of Science
Tokyo University of Science
1-3 Kagurazaka, Shinjuku-ku, Tokyo 162-8601, Japan

Keywords: ((liquid crystals, polymer-stabilization, molecular imprinting, templated self-assembly))

Self-organized nano- and microstructures of soft materials are attracting considerable attention because most of them are stimuli-responsive due to their soft nature. In this regard, topological defects in liquid crystals (LCs) are promising not only for self-assembling colloids and molecules but also for electro-optical applications such as optical vortex generation. However, there are currently few bottom-up methods for patterning a large number of defects periodically over a large area. It would be highly desirable to develop more effective techniques for high-throughput and low-cost fabrication. Here, a micro-pixelated LC structure consisting of a square array of topological defects is stabilized by photopolymerization. A polymer network is formed on the structure of a self-organized template of a nematic liquid crystal (NLC), and this in turn imprints other non-polymerizable NLC molecules, which maintains their responses to electric field and temperature. Photocuring of specific local regions is used to create a designable template for the reproducible self-organization of

defects. Moreover, a highly diluted polymer network (ca. 0.1 wt % monomer) exhibits instant on–off switching of the patterns. Beyond the mere stabilization of patterns, these results demonstrate that the incorporation of self-organized NLC patterns offers some unique and unconventional applications for anisotropic polymer networks.

Harnessing periodic nano- and micropatterns formed by the self-organization of soft materials is a promising approach for introducing emergent functionalities that are difficult to achieve using conventional lithographic techniques. To date, a great deal of effort has been devoted to exploring various systems such as block copolymers,[1] colloids,[2] and liquid crystals[3–6] for electronics, optics, and templating materials. Among these systems, nematic liquid crystals (NLCs) are the most suitable for electro-optical applications because of their intrinsic birefringence. Currently, the engineering of topological defects, which are ubiquitously observed in NLCs, has been attracting attention in research targeting colloidal assembly,[7] optical vortex generation,[8,9] and molecular self-assembly.[10,11] To realize these non-display applications, the precise control of the averaged molecular orientation, the so-called director, is essential. Although self-organization is the key to templating materials with low cost, high throughput, and molecular-level precision, it has proved difficult to spontaneously achieve uniform periodic patterns over a large area and creating complex director fields heavily relies on pre-patterned surfaces,[12–14] which require special devices. In this context, we have recently demonstrated an effective bottom-up approach to generate a reconfigurable square array of topological defects,[15] which are often referred to as “umbilics”.[16] The structure is induced by applying an AC electrical voltage to homeotropically aligned NLCs with negative dielectric anisotropy. (Figure S1, supporting information) The micro-pattern formation was achieved on a template-free fluorinated polymer (CYTOP, Asahi Glass Co.) surface simply by doping NLCs with an ionic compound. Although such a scalable “crystal-like” pattern has huge potential for optical applications, such as generation of multiple vortex beams[17–19],

micro lens arrays[20], polarization grating[21], and shape-programmable LC elastomers[22–24], some limitations of this system need to be overcome. First, the pattern formation is only possible for a specific class of NLC compounds, 4α,4′α-dialkyl-1α,1′α-bicyclohexyl-4β-carbonitriles (CCN-mn), which ensures both negative dielectric anisotropy ($\Delta\varepsilon < 0$) and homeotropic anchoring on the CYTOP surface. Particularly, the latter condition is difficult to realize because most NLCs show planar alignment. Besides, the CCN compounds possess low birefringence ($\Delta n \approx 0.03$),[25,26] which means that external fields cannot change the apparent birefringence over a wide range. Another point is that the reconfiguration of the pattern by epitaxial formation[15] is time consuming for device applications. To address these issues, we stabilized the pattern by mixing with a photocurable monomer.[27,28] To date, much effort has been devoted to polymer-stabilized liquid crystals (PSLCs) in various phases, such as the nematic,[29,30] cholesteric,[31,32] and blue phases.[33,34] However, compared with the other LC phases, the proposed applications of polymer-stabilized NLCs (PSNLCs) are limited, because in most experiments NLCs are used in unidirectional planar or homeotropic alignment, which tends to lead to light scattering caused by the random orientation of the director under electric fields.[29,35] Although complex director fields with periodic modulation are interesting for exploiting the unconventional use of PSNLCs, the study of PSNLCs with self-organized patterns has mainly concentrated on the stabilization of electroconvection[36,37] and the applied functionality has not been thoroughly explored. In this work, starting from a self-organizing micropattern of an NLC, we turned it into a polymer-stabilized template, and through simple photocuring of the structure, we show that the optical controllability and switching behavior of the patterned PSNLC can be improved significantly.

According to our recent findings,[15] here we used an NLC (CCN-37, Nematel) doped with 1 wt % of an ionic compound (tetrabutylammonium benzoate (TBABE), Aldrich) to generate a large number of topological defects. In addition, a bifunctional LC monomer (RM257, AK

Scientific) and a photoinitiator (Irgacure 651, Aldrich) were mixed. RM257 has a negative dielectric anisotropy and exhibits nematic phase in the range of 70-126 °C.[38] Thus, the mixed RM257 molecules align along the director of CCN-37. The mixed sample was introduced into a sandwich-type cell consisting of indium tin oxide (ITO)-coated glass substrates that were spin coated with an approximately 120 nm layer of CYTOP. To determine the experimental conditions, the solubility of RM257 into CCN-37 was examined together with the alignment of the mixed sample on the CYTOP surface. At room temperature (25 °C), the weight percent solubility amounts to approximately 10 wt %, above which point the sample needs to be heated. However, even if the sample is heated, a higher concentration of RM257 (≥15%) leads to a planar alignment. Considering that the temperature increase does not broaden the range of experimental conditions, in this work the polymerization was performed at room temperature unless otherwise noted.

As observed for CCN-37, the director reorientation by an AC electrical voltage, $V = V_0 \cos 2\pi f t$, leads to the formation of a square array of umbilics when the electrical voltage reaches a threshold. To perform the experiments efficiently, uniform defect arrays were prepared with the assistance of optical manipulation in the same manner as described previously.[15] V_0 and f, which are the amplitude and frequency, respectively, of the AC voltage required for the pattern formation, showed almost the same tendency as the sample not containing RM257 and Irgacure 651. The size of the grids, that is, the distance between the +1 umbilic and its −1 counterpart, was similar to the case where the polymerization components were not mixed. The entire area of the sample cell was cured using UV-LED light (365 nm) for 10 s with applying an electrical voltage.

Figure 1(a) shows a polymerized texture as observed by polarizing optical microscopy (POM) in the absence of an electric field. Here, in order to prepare a monodomain, an

electrical voltage was applied to a square region constructed from overlapping striped ITO electrodes, which works as a template for arranging defects. The edge of the electrodes helps align defects and the corner of the overlapped region uniquely determines the type of defects due to the fringe electric fields[15]. The pixelated grid-like (G) appearance under cross-polarized conditions was identical to that before polymer-stabilization, which implies that the RM257 molecules were oriented by the CCN-37 molecules. This stabilization was confirmed for the samples containing 0.5–10 wt % of RM257. For polymerized sample cells, the diffraction pattern could be readily generated as shown in **Figure 1(b)**, which was obtained using circularly polarized light. The details of the polarization properties will be reported elsewhere. The effect of temperature on a pixelated PSNLC is shown in **Figures 1(a)** and **(c)**–**(e)**, where all micrographs were obtained under the same illumination conditions. The thickness of the sample was 10.4 μm and the first-order yellow color was responsible for the low birefringence of CCN-37.[26] The retardation continuously decreased during heating (**Figures 1(c)**–(**e)**) without deterioration, indicating the controllability of the birefringence by temperature. The texture became dramatically darker at the nematic-to-isotropic phase transition of bulk CCN-37, although the G texture was still observable due to the anisotropic polymer network and the residual birefringence of CCN-37.[26] Importantly, when the temperature was sufficiently above the isotropic-to-nematic transition, RM257 irreversibly formed bundles and the resulting light scattering was observable by POM.[30] These bundles remained even after the sample was cooled to room temperature. **Figures 1(f)**–**(j)** show enlarged views of the bundled texture obtained under various illumination conditions. To permit better visualization, images were obtained using a thicker cell (22.6 μm). The temperature was set at 60 °C to ensure the isotropic phase of the bulk CCN-37. The two colors obtained by the insertion of a full-wave plate agree with the direction of the visualized director field. In contrast to the earlier work,[15] the polymer network demonstrated that umbilics with +1 defect strength are of the splay type.[16] Moreover, this indirect technique is

useful for understanding the director field in other complex regions, such as at dislocations formed by umbilics and at the corners of the electrodes, as shown in **Figures 1(k)** and **(l)**.

The grid-like RM257 network can be used as a template for imprinting other NLCs with the desired optical, electrical, and thermal properties. A conventional method for removing the non-polymerized LCs is to place the polymerized sample cell in an appropriate liquid solvent such as hexane.[39][40] However, despite our efforts, after washing it proved difficult for the refilled NLC to reproduce the same director field again. This could be because the polymer network had changed from the original configuration. Alternatively, the sample cell can be directly immersed in other NLCs[41] (**Figure 2(a)**). Here we show the results obtained using two typical NLCs (5CB with $\Delta\varepsilon > 0$, MBBA with $\Delta\varepsilon < 0$). We stress that keeping the nematic phase is crucial to infiltrate the NLCs without deterioration. Once the non-polymerized sample had undergone the transition to the isotropic phase, the indelible bundled texture appeared as in **Figure 1(g)**. Thus, the nematic-to-isotropic transition temperature must be considered. In our case, the transition temperature of the CCN-37/5CB mixture tends to decrease significantly, as shown in **Figure 2(b)**. This temperature dependence is useful to estimate the concentration of the mixture. The immersion of the sample cell with 5CB was performed at room temperature so that the diffusion proceeded in the nematic phase. The micrographs for the infiltration are displayed in **Figures 2(c)**–**(g)**. The concentration of RM257 was 7.1 wt %. The original texture of CCN-37 (**Figure 2(c)**) exhibited a first-order yellow color, while a significant color alternation was observed over time because of the enhanced birefringence by 5CB ($\Delta n = 0.17$) (**Figures 2(d)**–**(g)**). During the immersion, bundles such as those in **Figure 1(f)** did not appear under POM observation. This indicates that the 5CB molecules were well templated on the RM257 network that was originally templated by CCN-37. Next, we further show some methods to control the birefringence of the refilled NLCs by external fields. As shown in **Figure 2(h)**, the imprinted molecules

maintained the G texture when the temperature was varied. The replacement ratio of the 5CB can be estimated by the transition temperature of the CCN-37/5CB mixture. For the results presented, the transition temperature was 31 °C. According to the phase diagram (**Figure 2(b)**), this means that more than 90 wt % of 5CB can be replaced without light-scattering effects. Therefore, our approach allows the introduction of highly birefringent materials with $\Delta\varepsilon > 0$. This method is applicable to samples with lower concentrations of RM257, where the washout/refill method with liquid solvent would damage the network. An advantage of a low concentration of the polymer network is reorienting the director of the imprinted NLC molecules even after immersion. **Figures 2(i)** and **(j)** depict G textures immersed with 5CB and MBBA that contain 3.3 wt % and 1.6 wt % of RM257, respectively. For clarity, the experiments were performed in the early stage of diffusion from one edge of the cell, so that the first-order to second-order birefringence can be observed. POM micrographs taken under an application of an electrical voltage are shown in **Figures 2(k)** and **(l)**. Here we changed f to 10 kHz and V_0 was unchanged upon polymerization. In the case of 5CB, the behavior depends on the concentration. If the $\Delta\varepsilon$ of the mixture is positive, the electrical voltage makes the director perpendicular to the substrates. This can be clearly seen by comparing the left-hand sides of **Figures 2(i)** and **2(k)**, which show the decrease of the retardation. In contrast, the right-hand sides of **Figures 2(i)** and **2(k)** have $\Delta\varepsilon \approx 0$, and thus the textures appear similar. Contrary to 5CB, MBBA enhances the birefringence upon application of an AC voltage (**Figures 2(j)** and **(l)**). The dilute network easily reorients the director, while the texture does not show a noticeable change for higher concentrations (typically >5 wt %).

Another aim of this study was to install the defects at a desired position, especially in the homeotropic domain. This was achieved by using a focused laser beam to polymerize a local area of a sample cell. Here, as illustrated in **Figure 3(a)**, we present two examples of photocuring single defects (**Figures 3(b)**–**3(e))** and the square areas surrounded by them

(**Figures 3(f)**–**(i)**). The irradiation was performed after preparing the uniform G texture. A wavelength of 405 nm was selected after considering the absorption spectrum of RM257.[42] Once the polymerization is complete, the stabilized area can be confirmed by switching off the electrical voltage (**Figures 3(b)**, **(f)**, **(g)**). Clearly, single defects were stabilized regardless of the strength (**Figure 3(c)**). An important role of local polymerization is templated self-organization,[43] which can be demonstrated by applying electrical voltages because CCN-37 molecules in the non-irradiated area remain responsive to electrical voltages. **Figures 3(d)** and **(h)** were obtained under moderate voltages and **Figures 3(e)** and **(i)** under higher voltages. The connectivity of the polymerized and non-polymerized regions was quite smooth, leading to a highly reproducible texture (**Movie S1**, Supporting Information). In our system, no pre-patterning on the substrate is needed and the boundary (template) can be created as desired. Using these properties, for example, it is possible to switch the total number of +1 and −1 defects in the sample cell and localization of defects can be used for the shape-programmable systems if the structure is taken out from the cell as a free-standing film.

Because approximately 1 wt % of RM257 still stabilized the G texture, we further diluted the monomer concentration. When 0.1 wt % of RM257 was used, the G texture returned to the homeotropic alignment once the field was switched off. A surprising result was that the same texture could be obtained immediately after the electrical voltage was switched on. The switching of textures was repeatable (**Movie S2**, Supporting Information). To obtain the information on the polymer network, experiments were performed with a thicker cell gap. We were then able to recognize a slight birefringence of RM257 due to the increased retardation. This indicates that either the network was formed in the bulk even at such a low concentration or the localization of the network occurred near the substrate. Thus, the result is that a dilute polymer network, which however cannot maintain the G state, triggers the same texture by guiding the director along the network. The further importance of the polymer network was

confirmed by changing V_0 and f. **Figure 4** shows the boundary between the homeotropic and G states. The threshold curve exhibits the same tendency as observed in the sample without RM257. However, it can be seen that the G state can be observed over a broad frequency range from about 70 Hz to about 7 kHz. This is in marked contrast to the previous study, in which the G state was observable up to several hundred hertz. Remarkably, only a small V_0 was realized at high frequencies. We believe that this result offers a new use for a patterned PSNLC.

In conclusion, we have demonstrated that by polymerizing a self-organized LC pattern, it can function as a rapidly responsive, reproducible pixelated panel with a pixel size of a few micrometers to tens of micrometers, which is very small and thus allows high-resolution microdisplays and microsensor applications to be envisaged. We have also shown how the anisotropic polymer network can be used depending on the concentration. After polymerization, the imprinted molecules retain tunable electrical, optical, and thermal properties. The polymerization can also be applied to a local area. We believe our technique reported herein provides rich regular templates, which could be applied for new optical, electronic, and mechanical devices.

Experimental Section

Sample Cells: A standard sandwich-type LC cell is used for experiments. Indium-tin-oxide (ITO)-coated glass plates are spin-coated with an amorphous fluorinated polymer (CYTOP, Asahi Glass Co.). The film thickness is 120 nm.[15] For preparing LC samples, first we dope 4α,4'α-dialkyl-1α,1'α-bicyclohexyl-4β-carbonitriles ('CCN-37', Nematel) with 1 wt% of an ionic compound, tetrabutyl ammonium benzoate ('TBABE', Aldrich). The ion-doped CCN-37 is further mixed with a reactive monomer, 4-(3-acryloyloxypropyloxy)-benzoic acid 2-

methyl-1,4-phenylene ester ('RM257', AK scientific) and a photo-initiator, 2-2-dimethoxy-2-phenyl acetophenone ('Irgacure 651', Aldrich). The concentration of RM257 (0.1 – 10 wt%) and the photo-initiator (around 0.5 wt%) are calculated to the total mixture. All components are mixed in a chloroform solution. After using ultrasonic agitation, the sample is dried for 24 hours. The mixture sample is introduced into the cell and an AC voltage is applied. Texture observation is made under polarized optical microscopy (BX51, Olympus). For our optical manipulation experiments, an Nd-YAG laser (1,064 nm) focused through a microscope objective lens is irradiated to the sample cell on a motorized stage of an inverted microscope (IX71, Olympus).

Photopolymerization: Curing is made with UV-LED light (NS Lighting ULEDN-102CT, 365 nm in wavelength). The maximum power of the product is 4,000 mW/cm^2. In our case, the LED light is positioned at around 5 cm away from the sample cell and irradiation is made for 10 seconds under application of an electrical voltage. The intensity is several tens of mW/cm^2 to a few hundreds of mW/cm^2. Photopolymerization of a local area of the sample cell is made by a laser (405 nm, 20 mW) for several to ten seconds. After the power of the laser is reduced to 2 mW by a ND filter, the beam is focused by an objective lens (SLMPLN 50X, Olympus). The net power from the objective lens is ~0.001 mW. Considering the area of the irradiation, a crude estimation would be the order of hundreds of mW/cm^2.

Supporting Information

Supporting Information is available from the Wiley Online Library or from the author.

Acknowledgements

This work was supported by JSPS KAKENHI Grant Numbers (25103006, 16K17776) and by the Foundation for the Promotion of Ion Engineering.

Received: ((will be filled in by the editorial staff))
Revised: ((will be filled in by the editorial staff))
Published online: ((will be filled in by the editorial staff))

References

[1] H. C. Kim, S. M. Park, W. D. Hinsberg, I. R. Division, *Chem. Rev.* **2010**, *110*, 146.

[2] X. Ye, L. Qi, *Nano Today* **2011**, *6*, 608.

[3] D. K. Yoon, M. C. Choi, Y. H. Kim, M. W. Kim, O. D. Lavrentovich, H.-T. Jung, *Nat. Mater.* **2007**, *6*, 866.

[4] D. K. Yoon, Y. Yi, Y. Shen, E. D. Korblova, D. M. Walba, I. I. Smalyukh, N. A. Clark, *Adv. Mater.* **2011**, *23*, 1962.

[5] D. Coursault, J.-F. Blach, J. Grand, A. Coati, A. Vlad, B. Zappone, D. Babonneau, G. Lévi, N. Félidj, B. Donnio, J.-L. Gallani, M. Alba, Y. Garreau, Y. Borensztein, M. Goldmann, E. Lacaze, *ACS Nano* **2015**, *9*, 11678.

[6] Y. H. Kim, D. K. Yoon, H. S. Jeong, O. D. Lavrentovich, H. T. Jung, *Adv. Funct. Mater.* **2011**, *21*, 610.

[7] T. Araki, F. Serra, H. Tanaka, *Soft Matter* **2013**, *9*, 8107.

[8] E. Brasselet, N. Murazawa, H. Misawa, S. Juodkazis, *Phys. Rev. Lett.* **2009**, *103*, 103903.

[9] E. Brasselet, *Phys. Rev. Lett.* **2012**, *108*, 87801.

[10] X. Wang, D. S. Miller, E. Bukusoglu, J. J. de Pablo, N. L. Abbott, *Nat. Mater.* **2016**, *15*, 106.

[11] T. Ohzono, K. Katoh, J. Fukuda, *Sci. Rep.* **2016**, *6*, 36477.

[12] Y. Guo, M. Jiang, C. Peng, K. Sun, O. Yaroshchuk, O. Lavrentovich, Q. H. Wei, *Adv. Mater.* **2016**, *28*, 2353.

[13] H. Yoshida, K. Asakura, J. Fukuda, M. Ozaki, *Nat. Commun.* **2015**, *6*, 7180.

[14] C. Peng, Y. Guo, T. Turiv, M. Jiang, Q.-H. Wei, O. D. Lavrentovich, *Adv. Mater.* **2017**, 1606112.

[15] Y. Sasaki, V. S. R. Jampani, C. Tanaka, N. Sakurai, S. Sakane, K. V. Le, F. Araoka, H. Orihara, *Nat. Commun.* **2016**, *7*, 13238.

[16] A. Rapini, *J. Phys.* **1973**, *34*, 629.

[17] I. I. Smalyukh, D. Kaputa, A. V. Kachynski, A. N. Kuzmin, P. J. Ackerman, C. W. Twombly, T. Lee, R. P. Trivedi, P. N. Prasad, *Opt. Express* **2012**, *20*, 6870.

[18] P. J. Ackerman, Z. Qi, I. I. Smalyukh, *Phys. Rev. E* **2012**, *86*, 21703.

[19] B. Son, S. Kim, Y. H. Kim, K. Käläntär, H.-M. Kim, H.-S. Jeong, S. Q. Choi, J. Shin, H.-T. Jung, Y.-H. Lee, *Opt. Express* **2014**, *22*, 4699.

[20] Y. H. Kim, H. S. Jeong, J. H. Kim, E. K. Yoon, D. K. Yoon, H.-T. Jung, *J. Mater. Chem.* **2010**, *20*, 6557.

[21] S. P. Gorkhali, S. G. Cloutier, G. P. Crawford, *Opt. Lett.* **2006**, *31*, 3336.

[22] C. D. Modes, K. Bhattacharya, M. Warner, *Phys. Rev. E* **2010**, *81*, 60701.

[23] C. Modes, M. Warner, *Phys. Today* **2016**, *69*, 32.

[24] T. H. Ware, M. E. McConney, J. J. Wie, V. P. Tondiglia, T. J. White, *Science (80-.).* **2015**, *347*, 982.

[25] D. V. Sai, K. P. Zuhail, R. Sarkar, S. Dhara, *Liq. Cryst.* **2015**, *42*, 328.

[26] P. Oswald, G. Poy, A. Dequidt, *Liq. Cryst.* **2016**, *0*, 1.

[27] I. Dierking, *Adv. Mater.* **2000**, *12*, 167.

[28] I. Dierking, *Polym. Chem.* **2010**, *1*, 1153.

[29] R. A. M. Hikmet, *J. Appl. Phys.* **1990**, *68*, 4406.

[30] I. Dierking, P. Archer, *RSC Adv.* **2013**, *3*, 26433.

[31] R. A. M. Hikmet, H. Kemperman, *Nature* **1998**, *392*, 476.

[32] S. S. Choi, S. M. Morris, W. T. S. Huck, H. J. Coles, *Adv. Mater.* **2010**, *22*, 53.

[33] H. Kikuchi, M. Yokota, Y. Hisakado, H. Yang, T. Kajiyama, *Nat. Mater.* **2002**, *1*, 64.

[34] F. Castles, F. V. Day, S. M. Morris, D.-H. Ko, D. J. Gardiner, M. M. Qasim, S. Nosheen, P. J. W. Hands, S. S. Choi, R. H. Friend, H. J. Coles, *Nat. Mater.* **2012**, *11*, 599.

[35] R. A. . Hikmet, J. Lub, *Prog. Polym. Sci.* **1996**, *21*, 1165.

[36] N. Éber, P. Salamon, Á. Buka, *Liq. Cryst. Rev.* **2016**, *4*, 101.

[37] N. Mießen, J. Strauß, A. Hoischen, K. Kürschner, H.-S. Kitzerow, *ChemPhysChem* **2001**, *2*, 691.

[38] P. A. Kossyrev, J. Qi, N. V. Priezjev, R. A. Pelcovits, G. P. Crawford, *Appl. Phys. Lett.* **2002**, *81*, 2986.

[39] J. Guo, H. Cao, J. Wei, D. Zhang, F. Liu, G. Pan, D. Zhao, W. He, H. Yang, *Appl. Phys. Lett.* **2008**, *93*, 201901.

[40] V. K. Baliyan, V. Kumar, J. Kim, S.-W. Kang, *Opt. Mater. Express* **2016**, *6*, 2956.

[41] Y. Maeda, J. Kobashi, H. Yoshida, M. Ozaki, *Opt. Mater. Express* **2017**, *7*, 85.

[42] W. Zheng, C. C. Chan, *EPL (Europhysics Lett.* **2011**, *93*, 13001.

[43] A. Honglawan, D. A. Beller, M. Cavallaro, R. D. Kamien, K. J. Stebe, S. Yang, *Adv. Mater.* **2011**, *23*, 5519.

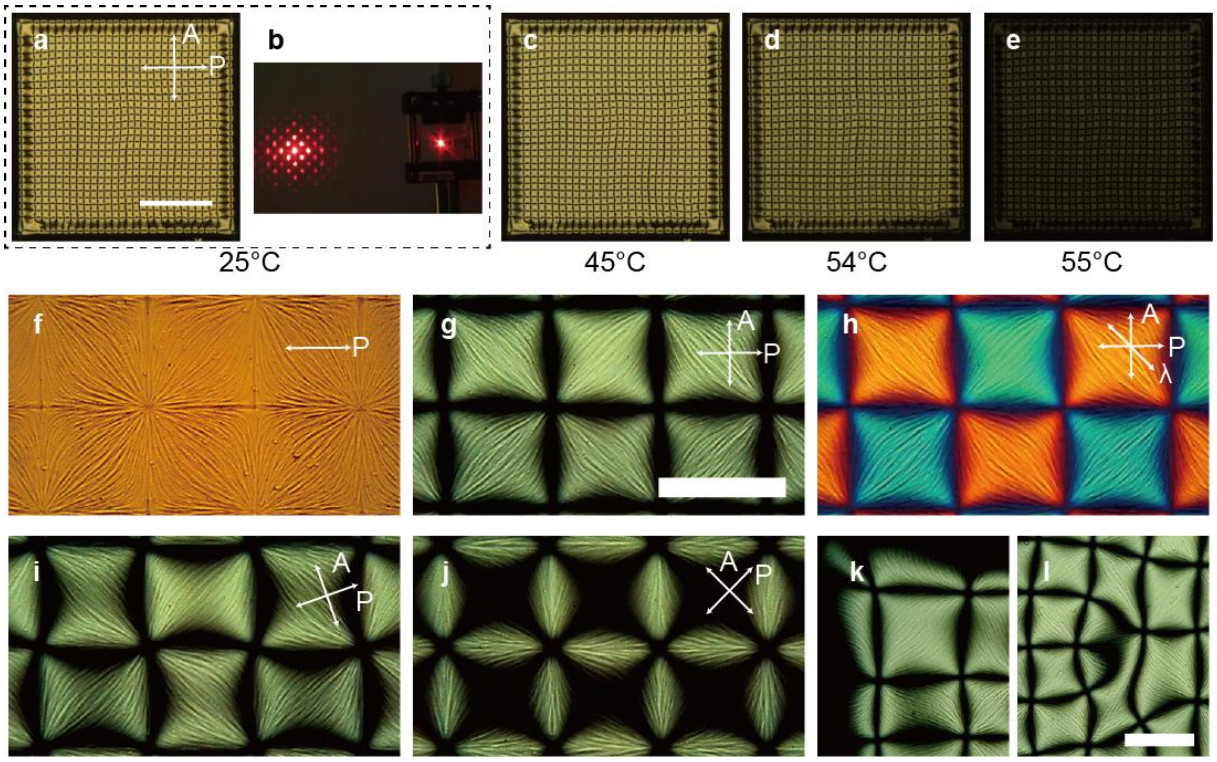

Figure 1. a) A polymer-stabilized G texture at room temperature of 25 °C. Scale bar 400 μm. The cell thickness is 10.4 μm. The concentration of RM257 is 7.1 wt%. The applied voltage is f=62 Hz, V_0=26.5 V. b) A diffraction pattern obtained by using a He-Ne laser. c)- d) The temperature dependence of the polymer-stabilized G texture: c) 45 °C, d) 54 °C, e) 55 °C. f)-j) Indirect visualization of the director field of G texture with bundled polymer network. Micrograph under f) plane polarized light, g) cross-polarized conditions and h) with a full-wave plate. i), j) Images taken by rotating the crossed-polarizers. k), l) Director configuration near a corner of electrodes and a dislocation of umbilics. The cell thickness is 22.6 μm for images f)-l). RM257 is 10.1 wt%. The applied voltage is f=37.5 Hz, V_0=26.5 V. Scale bars, 100 μm.

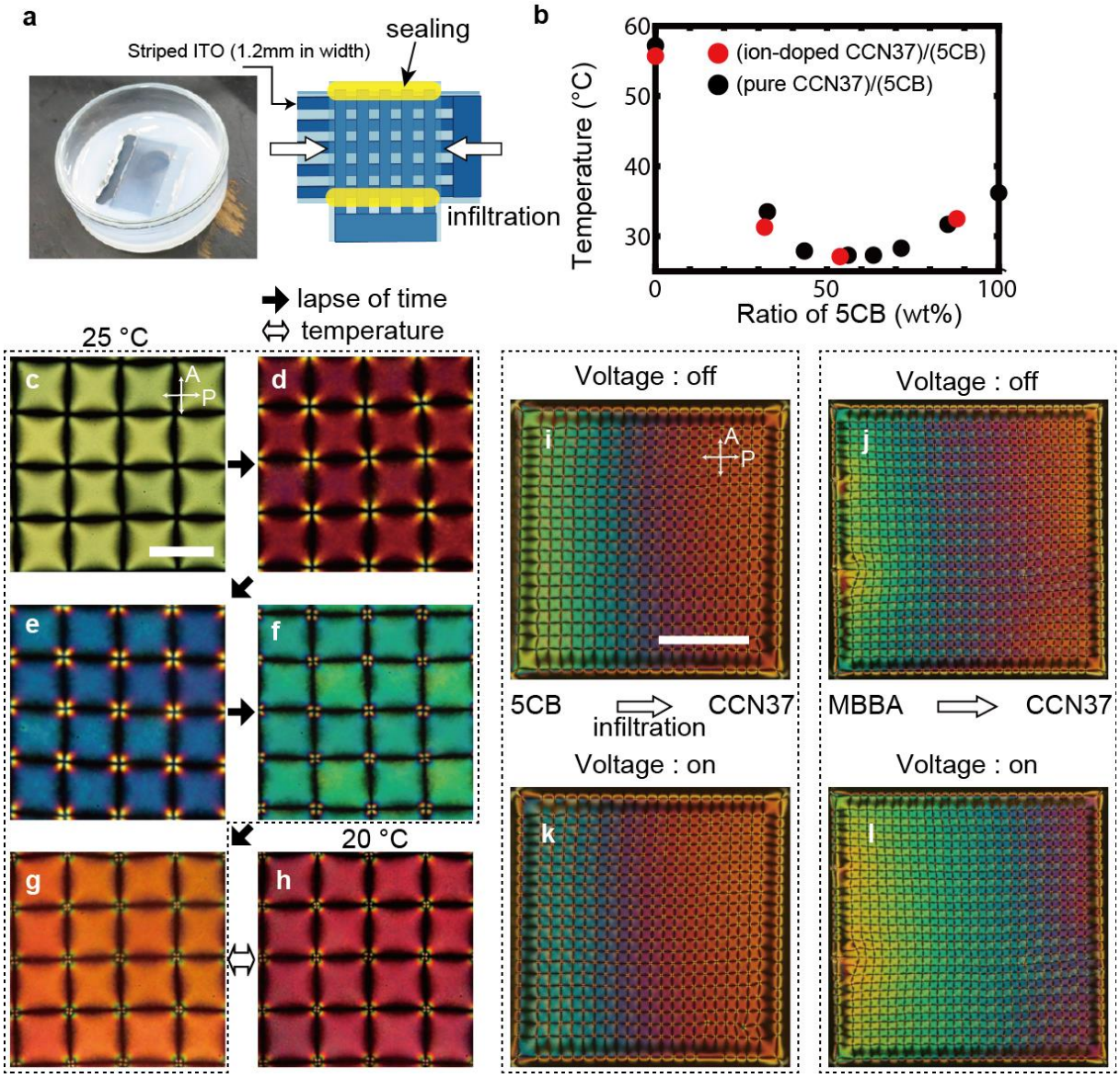

Figure 2. a) Schematic illustration of immersion experiment. b) Transition temperature to the isotropic phase of CCN-37/5CB mixtures. Black circles are for pure CCN-37. Red circles are for CCN-37 containing 1 wt% of TBABE. c)-g) Enlarged views of color alternation during time course as a result of immersion with 5CB. We note that the images c)-g) are taken at different locations of a cell because the process takes time (typically around a month). h) Enhanced retardation by decreasing temperature from g). i), j) POM images as a result of infiltration by 5CB and MBBA from left to right. RM257 concentration is 3.3 wt% for i) and 1.6 wt% for j). G-texture is polymerized at V_0=26.2 V. *f* is 50 Hz for i) and 90 Hz for j). k), l) POM images under the electric voltages of V_0=26.2 V, *f*=10 KHz.

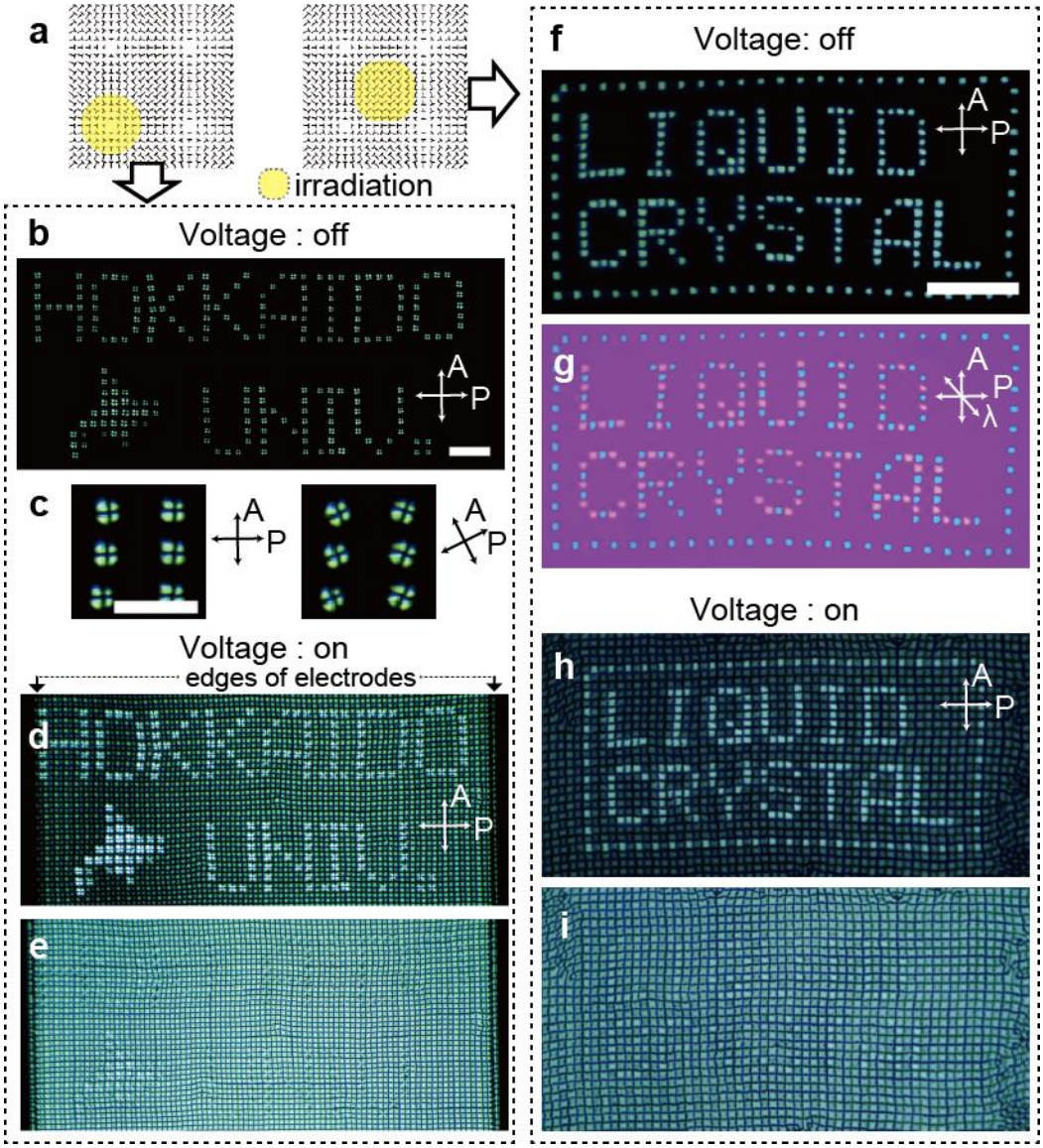

Figure 3. Application of laser irradiation for local polymerization. a) Schematic illustrations of photopolymerization of local areas. b) POM image of locally polymerized single umbilics. c) An enlarged view of b). d) POM image under a moderate voltage. e) POM image taken with sufficient voltage. f) A texture by polymerizing pixels instead of defects. g) Appearance with an insertion of a full wave plate. h) POM image under a moderate voltage. i) POM image under a sufficient voltage. The cell thickness is 3.8 μm. The concentration of RM257 is 7.1 wt%. Polymerization is made by a laser beam (405 nm) focused through an objective lens. The experiment is made with V_0=17.5 V and f=170 Hz. Scale bars, 100 μm for b),f) and 50 μm for c).

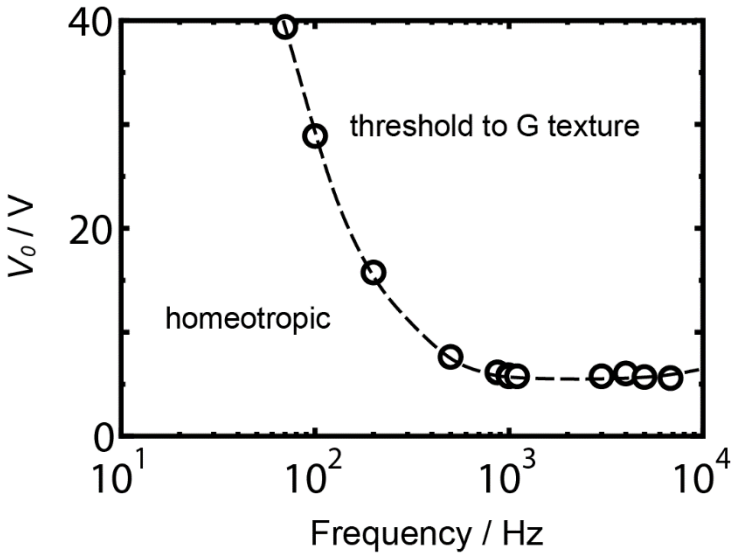

Figure 4. A dependence of the threshold voltage for a sample containing 0.1 wt% of RM257. The open symbols show the data showing the G pattern. The dashed curve is a guide to eyes. The cell thickness is 4.4 μm. The polymerization is made at V_0=26.2 V, 100 Hz.

,,
..

Supporting Information

Polymer-Stabilized Micro-Pixelated Liquid Crystals Tunable Optical Properties Fabricated by Double Templating

Yuji Sasaki, Motoshi Ueda, Khoa V. Le, Reo Amano, Shin Sakane, Shuji Fujii, Fumito Araoka, and Hiroshi Orihara*

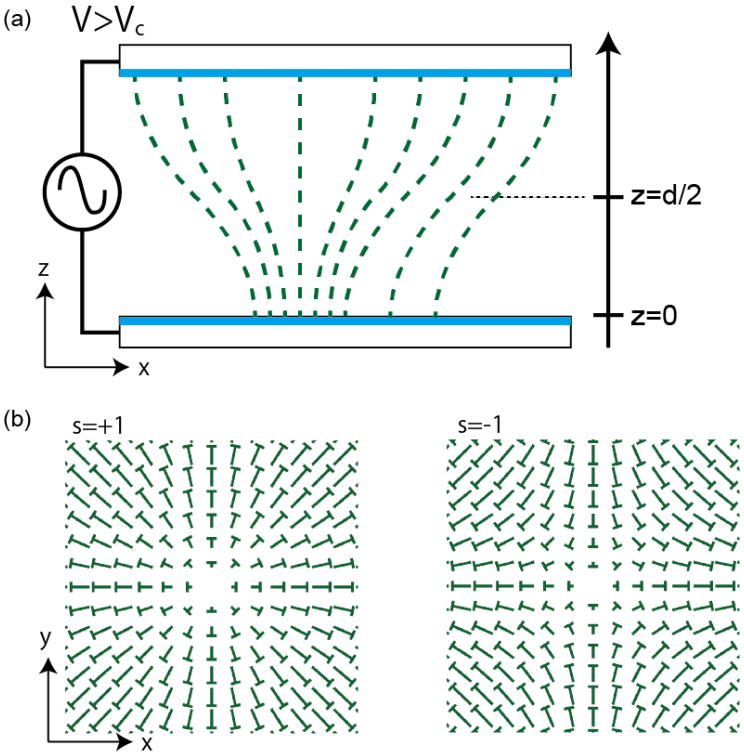

Figure S1. a) A cross-sectional view of the director field of umbilical defects above a threshold voltage V_c. The director aligns perpendicular to the substrates due the anchoring effect. The director at the mid-plane of the cell tends to tilt toward a horizontal (xy) plane due to the negative dielectric anisotropy. b) The director field of the umbilical defects projected in xy-plane at *z=d/2*.

Movie S1. A movie for a templated self-organization of umbilics. (real-time speed) Frist, a moderate electrical voltage is applied. After forming the uniform defects array, then the frequency of the applied electrical voltage is increased.

Movie S2. A movie for an instant on-off switching of the pattern. (real-time speed) The experiment is made for a sample containing 0.1 wt% of RM257. The same texture appears unless the polymer network is damaged.